

## **Ice Jam and Pileup Formations Against Piloti-Type Structures Caused by Tsunami Run-up with Sea Ice Floe**

Shinji Kioka<sup>1</sup>, Maiko Ishida<sup>1</sup>, Takahiro Takeuchi<sup>2</sup>

<sup>1</sup> Civil Engineering Research Institute for Cold Region, Sapporo, Japan

<sup>2</sup> Hachinohe Institute of Technology, Hachinohe, Japan

### **ABSTRACT**

When a tsunami occurs in icy waters, run-up waves carrying ice may cause greater damage than tsunamis without ice due to the static and dynamic forces generated by ice-floe-laden flows. We have conducted numerous model experiments simulating the onshore run-up of tsunamis containing sea ice floes, focusing on the formation of ice jams and pileups around land-based structures. This study specifically examines the effects of ice jams and pileups on a piloti-type structure, characterized by its ground floor supported by columns—a design often employed in tsunami evacuation facilities due to its presumed structural advantage against tsunami flows. The results show that after ice floes collide with the columns, the formation of ice jams and pileups between the columns dams the flow, resulting in significant static forces acting in the main flow direction. These forces are an order of magnitude greater than those observed in scenarios without ice floes. Additionally, a substantial vertical force, comparable in magnitude to the horizontal force, also acts on the structure. Our findings suggest that when designing structures with openings, such as windows or spaces between columns, the design forces for tsunami flow should not be reduced, as ice jams and pileups can significantly amplify the forces acting on these parts. Furthermore, we recommend evacuating to ground that is higher than is typically advised due to the potential for water level rise and ice pileups.

**KEY WORDS:** Tsunami, Ice pileup, Ice jam, Collision

### **INTRODUCTION**

For a tsunami that arrives at a coast, ice-bearing run-up waves may cause greater damage than ice-free run-up waves cause due to the static and/or dynamic action that occurs in ice-floe-laden flows. That is, ice floe pileups and jams may form in addition to the collision force imparted by the ice floes. Tsunami waves with sea ice floes have been reported to cause serious damage to private homes and bridges from the impact of the ice floes (e.g., Report of

the Tokachi-oki earthquake, 1954, Kagami, 2009)(see Fig.1). The run-up of sea ice to the shore and of river ice along rivers along with some minor damage to land structures caused by ice collisions were also confirmed during the 2011 Great East Japan Earthquake and Tsunami on the coast of the Kuril Islands (Kaistrenko, 2013). Sea ice run-up, river ice collisions with sluice gates, water surface elevation caused by ice-

related blockages (ice jams), and other phenomena also have been observed in Japan (Abe et al., 2014). At the end of 2017, Headquarters for Earthquake Research Promotion of Japan (HERP) estimates that there is between a 7 and 40 percent chance of an M-9 earthquake within the next 30 years along the Kuril Trench off Hokkaido, Japan, where quite a large tsunami is expected to arrive at ice-infested coasts. Accordingly, further efforts are required for research concerning ice-bearing tsunamis. Also, the thawing of permafrost due to recent climate changes, including in mountainous regions, is causing ground instability, raising concerns about landslides and the potential tsunamis that they may trigger. In recent years, significant landslides occurred in Ice Bay, Alaska, in 2015, and in Greenland in 2017 that generated massive tsunamis with waves on the order of several hundred meters high (USGS, 2018, Schiermeier, 2017). The latter of these tsunamis resulted in four fatalities and was a rare disaster involving ice. Thus, significant tsunamis may also occur in the Arctic Ocean due to factors other than earthquakes. Kioka et al. (2015, 2016, 2018) conducted model experiments involving the onshore run-up of a tsunami bearing sea ice floes, with a focus on ice jams and pileup formations between structures, and we examined the tsunami loads acting on the structures and the water depths around the structures in conditions with and without ice. The collision force and fracture mechanism of sea ice were also studied through medium-scale experiments and numerical calculations using 3-D discrete element model (DEM) (Kioka et al., 2010, 2012). In addition, a quasi-three-dimensional DEM has been developed that models tsunami run-up with ice floes with consideration of vertical motion to simulate ice pileup and ice jams (Kioka et al., 2019).

**Present study** addresses a piloti-column structure, i.e., one whose ground floor consists of pillars. This design has been applied to tsunami evacuation facilities due to its presumed structural advantages against tsunami flows. We conducted model experiments to investigate ice formations, such as ice jams and pileups, caused by tsunami flows around this piloti structure, and we examined the structure's effectiveness at withstanding regular tsunami flows and flows of ice-laden tsunamis, as well as examining design considerations in scenarios involving drift ice.

## MODEL EXPERIMENTS ON TSUNAMI RUN-UP WITH ICE FLOES

### Reviews of Previous Studies, and Points of Focus for This Experiments

Various risks that are additional to those of conventional tsunamis can be expected when sea ice floes are present, such as impacts of the floes against buildings/structures, as with tsunami debris, and the formation of ice jams and ice pileups. Ice jams have the potential to dam the inundation flow between onshore structures, thereby increasing the water level and causing greater forces to act on the structures. In the past, the ice jams that formed between the legs of

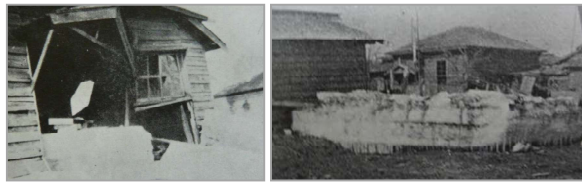


Figure 1. Run-up ice due to tsunami caused by the 1952 Tokachi-Oki Earthquake (Report of the Tokachi-oki earthquake, 1954)

jacket oil platforms have caused the platforms to collapse from increased drag force (Wang, 1983). At the time of the 2011 Great East Japan Earthquake and Tsunami, ice fragments piled up at river channels, jamming these channels and causing the water levels upstream to increase over the course of several days (Yoshikawa et al., 2012). We have conducted model experiments and have suggested the following mechanisms and processes as being behind the forces generated by ice-bearing tsunamis (see Fig.2, 11) (Kioka et al., 2018). After ice floes impart a collision force on structures, the tsunami flow is blocked by the formation of ice jams between the structures, and a large static force also acts on the structures because of the water level rise and because of hydrostatic pressure on the gaps between the structures (inter-structural spaces) due to the ice-jam. In other words, after the initial collision by ice floes, a quasi-steady state persists due to ice jams. Hereafter, the term "quasi-steady state" refers to a condition in which the ice and water are not completely stationary, but the magnitude of the forces and the changes in water level remain nearly constant. The ice jam formation depends on factors such as the flow conditions, the size of the ice pieces, and the spacing between structures (i.e., the size of the flow passage). If an ice jam does not form, it is considered that ice collisions will continue to occur. Even after the water subsides, the horizontal force caused by ice pileups remains, such as active earth pressure. It was confirmed that the active pressure and the residual force can be estimated by Rankine's earth pressure theory when ice fragments are regarded as Mohr–Coulomb materials. A simple theoretical model was also developed for estimating the water depth and the tsunami force imparted by tsunami run-up on structures using only the ratio of open area to total area as the parameter. This was instead of using the structure width and pitch. The simple theoretical model was developed by analogy to the occurrence of a negative bore caused by the sudden closing of a sluice gate (Kioka et al., 2015, 2018).

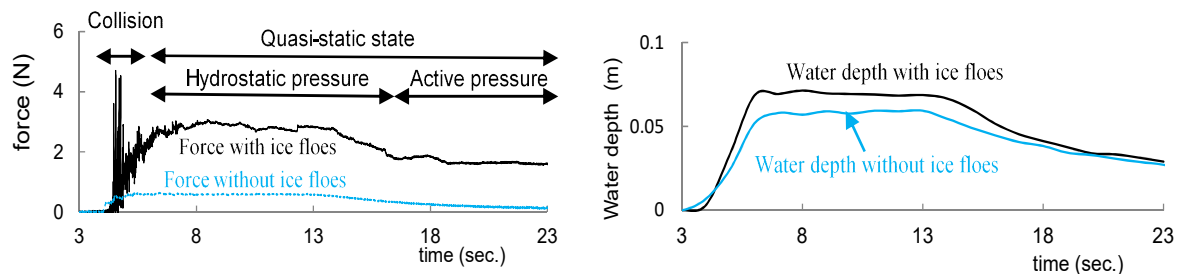


Figure 2. An example of the time-history of water depth in front of the structure and streamwise force on the structure under ice-jam formation, along with a comparison with the case without ice floes. These data were obtained from a model experiment with densely arranged onshore structures (Kioka et al., 2018)

In recent years, piloti structures have been considered advantageous in terms of resisting tsunami forces and are increasingly being adopted in tsunami evacuation facilities (Fig. 3). However, in cases with groups of sea ice or large amounts of drifting debris, risks similar to those involving ice jams can be anticipated. The experiments in this study focuses on these phenomena.



Figure 3. Examples of piloti structure applied to evacuation facility

Although the experimental method in this study is the same as that in a previous study (Kioka et al., 2015, 2018), it is described briefly here. As shown in Fig.4, a tsunami is generated by quickly opening the gate as in a dam break, under the condition where sea ice floes have drifted ashore, which then run up to level land after propagating up a uniform slope of 1/20 (scale: 1:100). On the landward side, an acrylic model of a piloti structure is placed that consists of staggered cylindrical columns each with a diameter of 10 mm, a height of 50 mm, and a center-to-center spacing of 100 mm, representing artificial ground or buildings (Fig. 4). Table 1 shows the main experimental conditions. The water storage depth ( $h_{0u}$ ) on the upstream side of the gate (0.12–0.22 m) was changed while the water depth downstream ( $h_{0d}$ ) remained constant. The ice floe models were made from rectangular polypropylene plates whose sides ranged from 1.5 cm to 10 cm in length, with a thickness of 5 mm. These were arranged such that the average side length was equivalent to 3 cm (3 m in full scale), according to the length distribution of sea ice floes along the Okhotsk Coast of Hokkaido (Kunimatsu et al., 1992). Although the density and the dynamic friction coefficient of the model ice are roughly the same as those of natural sea ice, the fracture strength and the elastic modulus of the model ice do not match dynamically at full scale. Therefore, evaluation of the collision force imparted by the ice floes was excluded. The collision force and the fracture mechanism of the ice were examined separately through a medium-scale experiment and numerical calculation (Kioka et al., 2010, 2012). While experiments with a given condition were conducted three times, we also made experiments without the onshore structure. We measured the forces acting on the structure with a sampling rate of 500 Hz using a three-component force meter. The force meter was attached to the top of the structure, aligned with its centroid, and a gap of 1 mm was left between the bottom of the structure and the ground. The natural frequency and the damping constant of the structure with the force meter were 32 Hz and 2.3%, respectively. Ultrasonic level gauges (Kenek Co., Ltd., type UH200, frequency response: 100 Hz) were used for measuring the run-up water depth (inundation depth onshore) so that the gauges would not impede the actions of ice floes. They were installed at



Model of piloti-structure	
Material	acrylic
Arrangement of columns	staggered cylindrical columns
Column diameter / center-to-center spacing	$\phi$ 10mm / 10cm
Model ice floes	rectangular polypropylene plates
	Specific density : 0.92
Storage depth $h_{bu}$ (m)	0.12, 0.17, 0.22
Water depth downstream of the gate $h_{od}$ (m)	0.07

the “position of slope change” and in front of and behind the structure. (The center of each sensor was set 8 cm upstream of the front face and 8 cm downstream of the rear face of the structure, so that the structure and the sensors would not interfere with each other.) The water depth was visually observed at 1-sec intervals by digital video cameras placed at the same positions as the gauges, because accurate measurement by only gauges was thought to be difficult, especially in case with ice floes. Also, the run-up flow velocities (inundation velocities onshore) were measured by electromagnetic velocity meters (Ketek Co., Ltd., FM2001H, frequency response: 20Hz), which were able to be embedded on the floor. Such meters do not disturb ice floe run-up, and they can reduce electrical noise because they are always covered with a thin film of water. Because if a meter that is exposed to the air is suddenly inundated, noise is assumed to be generated.

## EXPERIMENTAL RESULTS AND DISCUSSION

### General Trends

First, the characteristics of the incident waves without ice floes or structures in this experiments are briefly explained. In this experiments, the downstream water depth ( $h_{0d}$ ) was fixed. However, preliminary experiments that included changes in water depth had already been conducted to investigate the characteristics of the incident waves. Fig. 5 shows the characteristics of the incident waves along with the results of this experiments and the results of previous studies (Kioka et al., 2013). The water depth and flow velocity on land increased with the water storage depth ( $h_{0u}$ ). It was presumed that these values were determined primarily by the difference between the water storage depth ( $h_{0u}$ ) and the land elevation, regardless of the downstream water depth. This observation can be explained using the analogy of a broad-crested weir, assuming the “position of slope change” as the control section (Kioka et al., 2013). Additionally, the time-dependent changes, not only the changes in the quasi-steady state but also those in the tsunami front, were observed to remain approximately the same regardless of the downstream water depth ( $h_{0d}$ ). Under quasi-steady conditions, the Froude number at the onshore area (near the structure) was estimated to be 0.76 to 1.1 from the flow velocity and water depth. Hereinafter, the run-up water depth is defined as the incident water depth ( $h_0$ ). Furthermore, even with structures, the water depth at the position of slope change (in the quasi-steady state) was found to roughly correspond to  $h_0$  until the waves that were reflected back by the structure reached that position.

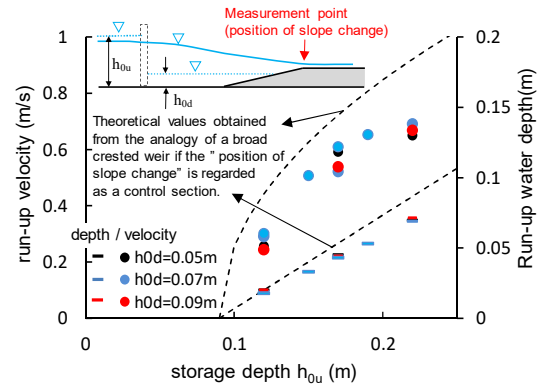


Figure 5. Characteristics of Time averaged incident waves during quasi-steady state. These results are for waves without ice floes or structures.

### Characteristics of the Tsunami around a Structure with Ice Jams

Figs. 6(a) - (c) show the run-up water depth and the streamwise and vertical forces acting on the entire structure, respectively, with ice jams, as a function of the water storage depth. The



run-up water depth, whose measurements are relatively low in noise, was measured using an ultrasonic water level gauge at the position of slope change for reasons that will be described later. The ensemble average of three measurements is shown in the figure. The water level without ice floes (the dotted line) is shown in Figure (6a). The load measurements were filtered using a 30-Hz low-pass filter, and a representative measurement from the three trials is shown in order to visualize the collision force imparted by the ice floes. Fig. 7 shows an example for  $h_{0u}=17\text{cm}$ , with the time series variations in the run-up velocity, water depth, and loads acting on the structure during the period when ice jams were forming, along with a comparison to the case without ice floes. (The loads are evaluated as ensemble averages, primarily to compare the loads in a quasi-steady state.) The figure also includes the measured flow velocity and the water level with neither the ice floes nor the structure. Fig. 8 shows

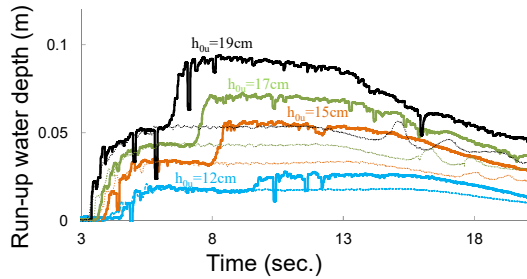


Figure 6(a) Time variation of run-up water depth with (solid line) and without (dotted line) ice jam formation

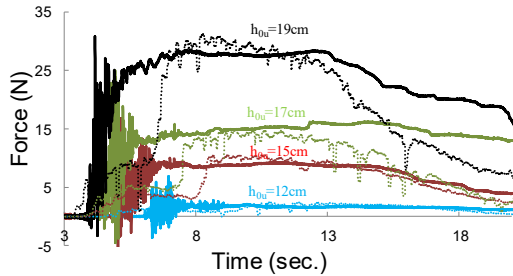


Figure 6(b) Time variation of streamwise force on entire structure under ice jam formation. Dotted lines indicate estimated values by hydrostatic model.

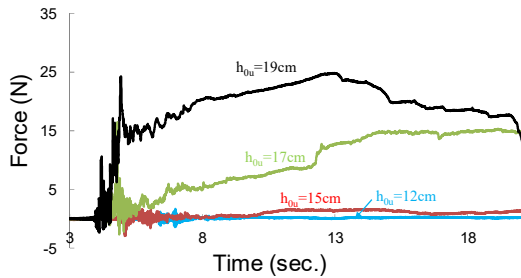


Figure 6(c) Time variation of vertical force on the entire structure with ice jam formation

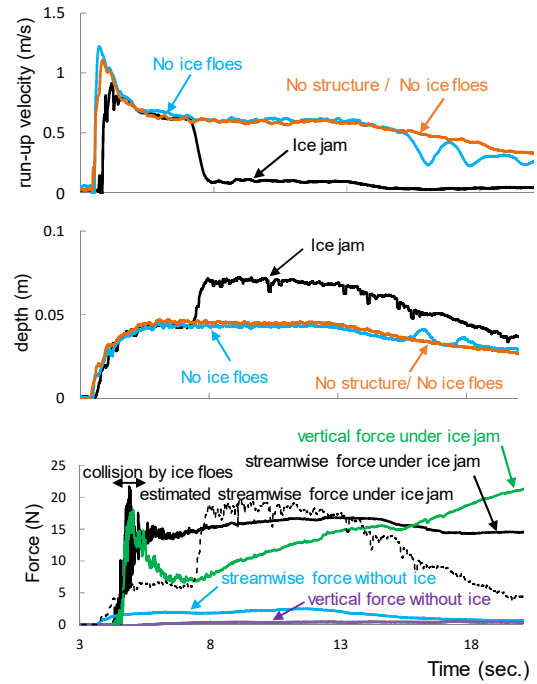


Figure 7. An example of time-series variations in run-up velocity, water depth, and force on structure during ice jam formation, along with a comparison to the case without ice [ $h_{0u}=17\text{cm}$ ]

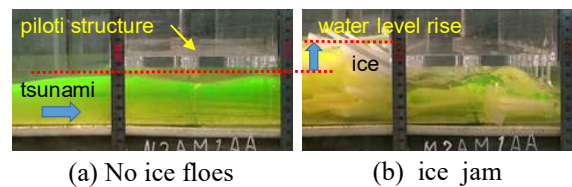


Figure 8. Images of conditions near structure during steady states with and without ice jam formation, corresponding to Fig. 7 [ $h_{0u}=17\text{cm}$ ]

images of the conditions near the structure during steady states with and without ice jams, corresponding to Fig. 7. The front view with ice jams has already been presented in Fig. 4. Furthermore, Figs. 9 and 10 illustrate the relationships between the run-up velocity, the run-up water depth normalized by the incident water depth ( $h_0$ ), evaluated as time averages during the quasi-steady state.

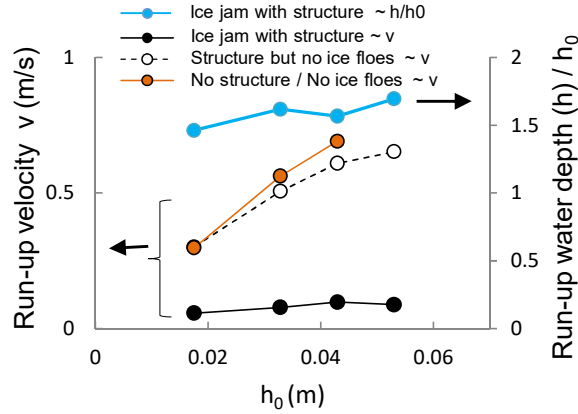


Figure 9. Relationship between run-up velocity, water depth and incident water depth ( $h_0$ ), evaluated as time averages during the quasi-steady state. These figures also compare the cases with and without ice jam formation.

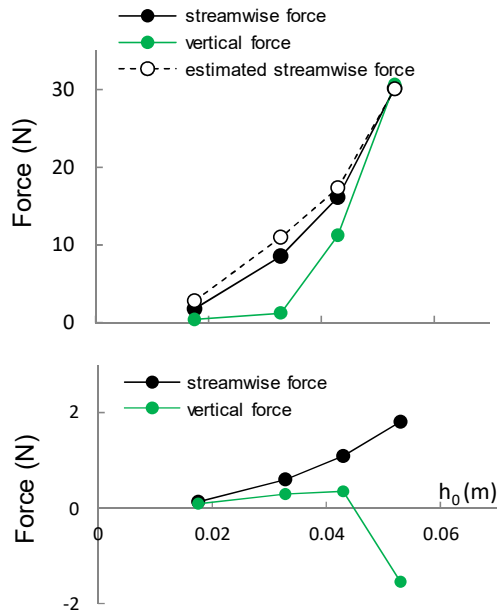


Figure 10. Relationship between streamwise force, vertical force and incident water depth ( $h_0$ ), evaluated as time averages during quasi-steady state. The upper and lower figures indicate the cases with and without ice floes, respectively.

during the quasi-steady state. These figures also compare the cases with and without ice jams.

First, we consider the run-up water depth. These measurements were obtained using an ultrasonic water level gauge, which estimates the water depth by measuring the distance from the sensor in the air to the water surface. With ice floes, significant errors and noise are a concern due to ice floes extending above the water surface. However, at the position of slope change (Fig. 6(a)), although some noise was observed, the measurements were found to be consistent with visual observations, yielding reliable results. The run-up water depth at the position of slope change with ice floes exhibited a stepped variation. This is due to the ice jams between the pillars of the structure, which obstructed the flow and generated reflected waves (negative-surge waves). In contrast, without ice floes (the dashed line), no reflected waves were generated, and the water depth closely matched the first step observed with ice floes. Furthermore, as shown in the upper part of Fig. 7, this architectural structure maintains a water level close to that observed without the structure, indicating the advantage of a design that results in minimal water level rises. However, when ice floes or other drifting debris cause blockages (jams) between the pillars, the flow is obstructed, leading to a significant rise in the water level upstream of the structure. This elevated water level is maintained in a quasi-steady state (defined here as a state where water level, flow velocity, and forces exhibit minimal temporal variation) and can exceed 1.5 times the water depth observed without ice floes. (Refer to the second step in Fig. 6(a) and Fig. 9.)

Regarding the flow velocity (Figs. 7 and 9),

it peaks with the arrival of the tsunami. Without ice floes, the flow velocity is similar to that observed without the structure. With ice floes, the flow velocity matches that of the former case until the reflected wave arrives, after which the velocity drops sharply. This change in flow velocity is observed to inversely correspond to the changes in water level. However, as noted in a previous study (Kioka et al., 2015), the cross-sectional area of flow can be reduced due to water blockage caused by ice floes, potentially causing localized increases in flow velocity. This phenomenon requires attention due to the risk of scouring near the base of the structure.

Next, we consider the streamwise force (Figs. 6(b), 7, and 10). Without ice floes, the streamwise tsunami force acting on the entire structure is reduced, indicating that the piloti structure effectively mitigates tsunami forces. However, with ice floes, a large collision force is first imparted by the ice floes, followed by a significant quasi-steady (quasi-static) force that is at least one order of magnitude greater than the streamwise force in the absence of ice floes. The force in the quasi-steady section is mainly attributed to the water level rise and the hydrostatic pressure caused by the water mass trapped between the columns (See Fig. 11). These trends are consistent with those observed in a previous study (Kioka et al., 2018) under the condition where several prism-shaped structures were arranged horizontally on land. The streamwise force acting on the entire structure is evaluated using the following equation.

$$F = \frac{1}{2} \rho g B (h_1^2 - h_2^2)$$

In this case,  $B$  represents the width of the entire structure (which is the width of the channel), and  $h_1$  and  $h_2$  are the water depths on the upstream and downstream sides of the structure, respectively. As shown in Figs. 8 and 11, since the water surface decreases right in front of the structure through the ice floes,  $h_1$  is taken as the water depth at a stable point farther upstream (the position of slope change). In other words, the hydrostatic pressure slightly upstream of the structure is assumed to act on the structure through the ice floes. The estimated forces in the quasi-steady state (the dashed line) based on this model are shown in Figs. 6(b) and 10, and they closely agree with the experimental values in the steady state. However, as shown in Fig. 6(b), the estimated forces obtained by the above hydrostatic theory do not match the experimental values for forces, except in the steady state. In addition to the steady state of hydrostatic pressure, the measured values consist of an initial added collision force, followed by a load that decreases more gradually than the hydrostatic pressure after the steady state, which seems to be a residual force that is not zero. This load is interpreted as the active pressure (earth pressure) caused by the ice floes that becomes apparent as the water level decreases. These trends are also consistent with those observed in a previous study, and Fig. 11 outlines the concept behind the action of force with ice (Kioka et al., 2018). Therefore, even when the water level decreases to the point where it becomes negligible, it is necessary to consider that the ice floes continue to impart active pressure on the structure.

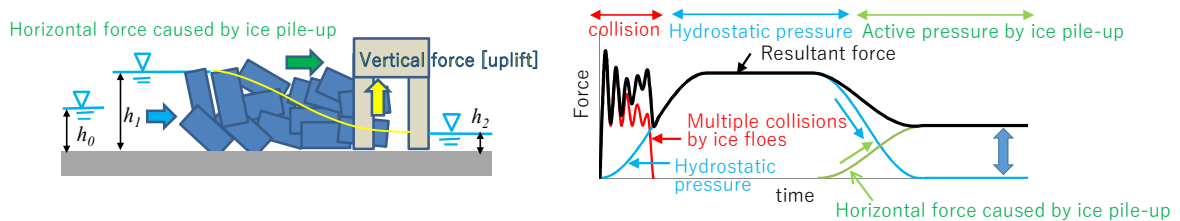


Figure 11. Model for action process of tsunami force with ice floes



Focusing next on the vertical load (Figs. 6(c), 7, and 10), it is evident that, particularly when the water storage depth or the runup water depth is great, the vertical load can be of the same order of magnitude as the streamwise force. Moreover, the temporal variation in vertical load is complex: while the streamwise load tends to stabilize during the steady state, the vertical load exhibits various behaviors, such as continuing to increase, rising further after reaching the steady state, or conversely decreasing. These behaviors are likely influenced by factors such as the buoyancy of the ice floes, their degree of clogging, and their arrangement, although the detailed mechanisms remain unclear. In contrast, without ice floes, the vertical load is limited to the buoyancy at the base and is minimal. However, at  $h_{0u}=19\text{cm}$ , the vertical force shifts downward, which is presumed to result from negative pressure caused by the water surface flowing very close to the ceiling. In any case, with ice jams, a significant vertical upward load, comparable to the streamwise load, simultaneously acts on the structure. This highlights the necessity of paying sufficient attention to pullout, overturning, and other risks to structures.

## CONSIDERATIONS FOR BUILDING DESIGN AND DISASTER PREVENTION

In the case of tsunamis accompanied by large amounts of drifting objects or debris such as sea ice, there are potential risks not only from their collision but also from additional hazards, particularly for piloti buildings. These risks include blockages (ice jam formations) or pileups of drifting objects in the gaps between the columns of such buildings or between adjacent buildings. This can lead to the damming of water flow, causing a significant rise in water levels on the upstream side of the building. As a result, large hydrostatic loads in the main flow direction act on the structure. Additionally, the damming effect may locally increase the flow velocity, necessitating careful attention to potential scouring near the base of the structure (Kioka et al., 2015).

For economical design, proposals have been made to reduce the design forces for tsunami flow in piloti structures or in facilities with openings such as windows. However, in regions prone to significant amounts of tsunami debris, including timber, vehicles, containers, and ice floes, the risk of jams must be carefully considered, and the design forces for tsunami flow acting on such parts should not be reduced.

Furthermore, it is important to note that, in addition to the forces in the main flow direction, equally significant upward vertical forces may act simultaneously. Even after the water level recedes, horizontal loads caused by accumulated drifting objects may persist. In addition to such loads, the rise in water level and the pileup of ice floes may require evacuation to higher ground than that for ordinary tsunamis.

## CONCLUSIONS

This study focused on piloti buildings, which are considered advantageous against tsunami forces and are used as tsunami evacuation facilities. Through model experiments, we investigated the impact and risk of run-up tsunamis with sea ice and clarified their effects. Additionally, we proposed key considerations for building design and disaster prevention in regions prone to significant amounts of tsunami debris such as sea ice. The main findings are summarized below.

(1) When ice floes are not present, the flow velocity and run-up water depth near the building are found to be approximately the same as those without the building. Additionally, the tsunami force acting on the entire building in the main flow direction was less without ice than with ice. These findings confirm that piloti structures are effective against tsunamis when ice or large amounts of drifting debris are not present.

(2) However, when ice floes are present, they form blockages (ice jams) between columns, damming the flow and causing significant rises in water level on the upstream side of the building. The water depth can exceed 1.5 times that of the ice-free case. Regarding tsunami forces, large initial collision forces are imparted by the ice floes, followed by a quasi-steady load that remains considerably high. The sustained load in the main flow direction is an order of magnitude greater than in the ice-free case, primarily due to the increased water level and the hydrostatic pressure from the dammed water mass between the columns.

(3) Furthermore, a significant upward vertical load, comparable in magnitude to the load in the main flow direction, was found to act simultaneously. This suggests that sufficient attention should be given to the risks of uplift and overturning.

(4) Based on the findings of this study, it is recommended that when piloti structures or facilities with openings such as windows are designed in areas with large amounts of drifting debris, including sea ice, the design forces acting on such parts should not be reduced. This recommendation is for safety. Additionally, for evacuation, the rise in water level and the pileup of ice floes may require evacuation to higher ground than for ordinary tsunamis.

As a future task, since the ice models used in this study were rectangular blocks, we should conduct experiments using models of various shapes. We also plan to clarify the conditions under which ice jams form by considering various factors such as tsunami or current conditions and structural configurations.

## REFERENCES

Abe, T., Yoshikawa, Y., Satoh, Y., Itoh, A. and Yamaguchi, S., 2014. Research on the effects of river tsunami with ice floes on structures, *Proc. 22nd IAHR International Symposium on Ice*, pp.671-678.

Kagami, Y., 2009. DAMAGE ARTICLES APPEARED ON LOCAL NEWSPAPERS IN HOKKAIDO-Literature survey of the off Nemuro earthquake of March 22, 1894 Part 2-, *AIJ J. Technol. Des.* Vol. 15, No.31, pp. 951-954. (in Japanese)

Kaistrenko, V., 2013. Manifestation of the 2011 Great Tohoku Tsunami on the Coast of the Kuril Islands: A Tsunami with Ice, *Pure Appl. Geophys.*, 170 (6-8), pp. 1103-1114.

Kioka, S., Yamamoto, Y., Sugawara K., Endo, T. and Takeuchi, T., 2010. Medium-scale Experiment and Numerical Simulation using 3-D DEM for the Impact Load by an Ice Floe against a Pile Structure, *Proc. 20th IAHR International Symposium on Ice*, No.110.

Kioka, S., Takeuchi, T. and Kanie, S., 2012. Medium-scale Experiment and Numerical Simulation for the Impact Load by an Ice Floe against a Pile Structure, *J. JSCE, Ser. A2 (Applied Mechanics)*, 68(2), pp.423-432.

Kioka, S., Mori, M., Endo, T., Takeuchi, T. and YATANABE, Y., 2013. A Study of Tsunami Inundation Flow with Ice Floes in Urban Area, *Proc. civil engineering in the ocean, JSCE*, 69 (2), pp.509-514. (in Japanese)

Kioka, S., Takeuchi, T. and Watanabe, Y., 2015. Characteristics of Sea Ice floes Run-up caused by Tsunami Considering Ice Jams and Ice Pile-ups around Structures, *Proc. 25th International Offshore and Polar Engineering Conference (ISOPE)*, 3, pp. 778-782.

Kioka, S., Takeuchi, T. and Maruta, N., 2016. Fundamental Study for Physical Experiments and Numerical modelling of Ice-Jams and Ice Pile-ups Driven by Run-Up Tsunami Wave, *Proc. 23th IAHR International Symposium on Ice*.

Kioka, S., Ishida, M. and Takeuchi, T., 2018. Experimental and theoretical considerations on water depth and force on onshore structures driven by run-up Tsunami wave in ice-infested waters, *Proc. 24th IAHR International Symposium on Ice*, pp.359-369.

Kioka, S., Ishida, M. and Takeuchi, T., 2019. NUMERICAL SIMULATION OF DRIFTING AND RUN-UP ICE FLOES DRIVEN BY TSUNAMI, *Proc. of ASME 2019 38th International Conference on Ocean, Offshore and Arctic Engineering (OMAE2019)*, Paper No: OMAE2019-95901.

Kunimatsu, S., Hara, F., Takahashi, Y. Saeiki, H., Enoki, K. and Imaizumi, A., 1993. Study on size of drift ice at the Okhotsk Sea Coast of Hokkaido, *Proc. of civil engineering in the ocean, JSCE*, 9, pp.95-100.

Research Committee of the Tokachi-oki earthquake.1954. Report of the Tokachi-oki earthquake ( in Japanese)

Schiermeier, Q., 2017, Huge landslide triggered rare Greenland mega-tsunami, Nature News, Published: 27 July 2017, doi:10.1038/nature.2017.22374.

US Geological Survey, Landslide hazards. 2018, Mountain Permafrost, Climate Change, and Rock Avalanches in Glacier Bay National Park, Alaska,

<https://www.usgs.gov/programs/landslide-hazards/science/mountain-permafrost-climate-change-and-rock-avalanches-glacier>, Jun.18, 2018 (Accessed 5 Feb.2022).

Wang, Q.J., 1983. A Tentative View on Ice Load Applied on Jacket Platforms in Bo-hai Gulf, *Proc. International Conference on Port and Ocean Engineering under Arctic Conditions (POAC)*, 2, pp. 930-939.

Yoshikawa, Y., Abe, T. and Hirai, Y., 2012. Simulation of Ice Jam generated by Tsunami in the Mu River, J. *JSCE, Ser. B2 (Coastal Engineering)*, 68 (2), pp.416-420.